1 Structure of non-polymeric glasses

1.1 Overview

The principal assignment of this book is to present the physics of inelastic deformation and fracture of polymers, incorporating microstructural forms ranging from fully disordered glassy polymers to semi-crystalline morphologies of quite considerable crystalline perfection. While the semi-crystalline polymers have few, if any, parallels in morphology among other solids, the glassy polymers have such parallels in their atomic packing forms and morphologies in metallic glasses and space-network glasses, which exhibit most of the forms of structural relaxation, inelastic response, and fracture behavior of glassy polymers, albeit often in modified forms and on somewhat different scales. Since these non-polymeric glasses are free of the severe molecular-segmental-level topological constraints, they exhibit the corresponding forms of mechanical response in a far simpler context, which is amenable to more precise analysis. For this reason we start our assignment in this chapter by considering in some depth the hierarchical details of atomic-packing forms of metallic glasses and those of amorphous silicon as a surrogate for a space-network glass before we deal with the molecular structure of glassy polymers and semi-crystalline polymers in Chapter 2. The atomic structure of amorphous silicon, in particular, makes contact with other directionally bonded covalent glasses and acts as a bridge between the densely packed amorphous metals with close-to-isotropic atomic interaction and high levels of atomic coordination and the structures of randomly snaking chain molecules of polymer glasses.

In both cases, namely for amorphous metals and for space-network glasses, in this chapter we develop important concepts such as free volume or liquid-like atomic environments that both serve to promote structural rearrangements and also play crucial roles in triggering shear relaxations under stress that can range from few-atom clusters to far-reaching avalanches of plastic events. In every case, however, the presentation of the quantitative details of the topology and kinetics of such relaxations will be deferred to later chapters, where they are discussed together with the corresponding phenomena in glassy polymers, using the simpler processes in amorphous metals as guides to the more complex processes in polymers. For metallic glasses, in which crystallization is suppressed and replaced by disorder, or at best only by some short-to-medium-range order, the

characteristic atomic packing can be reached operationally in a variety of ways. These include, e.g., direct condensation from a vapor into a solid and irradiation of a crystalline solid by energetic particles at relatively high fluences at low temperatures at which reordering of knock-on atoms is largely suppressed. However, the most widely used route for obtaining a metallic glass is by rapid cooling of a complex alloy melt that is fast enough to override crystallization. It is this route that will be of exclusive interest to us.

The first report of a metallic glass was that by Duwez and co-workers concerning an Au–Si alloy (Klement *et al*. 1960). Since that time the science and technology of the production of the metallic glasses has progressed from a scientific curiosity to a very active area of materials science, leading to the development of a myriad of increasingly more stable glasses with wide-ranging potential for product applications.

To understand the thermodynamics and kinetics of formation of metallic glasses through rapid cooling of an alloy melt of complex composition by overriding crystallization, a number of interrelated subjects need to be understood in considerable detail. These include the evolving changes in atomic packing in sub-cooled melts, the kinetics of inter-diffusion of the constituent atom species that are part of the kinetics of atomic relaxations in the sub-cooled melts entering the glass transition range, and the kinetics of the competing crystallization processes.

In the following sections we discuss first the atomic packing in sub-cooled alloy melts near a glass transition, referring to results obtained from recent combinations of modeling studies and associated experiments for some successful alloy compositions of metallic glasses. We follow this by considering the kinetics of structural relaxations in some metallic glass compositions supported by actual inter-diffusion experiments on constituent atom species. We contrast these observations with competing forms and kinetics of polymorphic crystallization processes in these compositions to arrive at classical time–temperature–transformation (TTT) diagrams. Following these considerations of the structure of sub-cooled alloy melts, we consider the all-important process of glass transition from a point of view of cessation of percolation of unit structural relaxation elements of atomic clusters possessing liquid-like character. Finally, employing mechanistic considerations and their kinetics, we examine some very successful metallic glass compositions that now permit one to obtain metallic glasses in relatively bulky form with sufficient stability in the sub-cooled melt to permit increasingly complex processing paths.

We follow the discussion of metallic glass alloys with a brief parallel consideration of the behavior of amorphous silicon that is based primarily on computer simulations that have not only introduced the corresponding behavior of space-network glasses but also permitted a much deeper mechanistic understanding both of structural relaxations, and, more importantly, of the nature of plastic shear relaxations by ubiquitous shear transformations in glassy solids of all types, particularly in glassy polymers. These are developed in detail later in Chapters 7 and 8.

1.2 Glass formability in metallic alloys

The requirements for glass formability in metallic alloy melts by rapid quenching have received much attention since the first report by Duwez and co-workers in 1960 on obtaining a metallic glass in an Au–Si alloy composition. Both laboratory experiments and computer studies have established that melts of pure metals tend to crystallize at such high rates that they cannot be quenched rapidly enough to obtain a glass. Thus, obtaining an alloy glass requires satisfying a number of interrelated conditions that stifle crystallization. Success in the early investigations with binary metal–metalloid compositions of, e.g., Au–Si, Pd–Si, Fe–B, etc. with atom number ratios of 4:1 between metal and metalloid ions of substantial atomic-size difference already demonstrated the importance of atomic-size difference between constituents to stabilize the melt and retard crystallization. Other related factors that emerged as essential for glass formability include the presence of a deep eutectic in the alloy composition that is beneficial in shortening the path between the melt and the glass; a high viscosity of the sub-cooled alloy melt at the liquidus range; and well-chosen alloy constituents requiring complex polymorphic crystallization involving coupled, sluggish diffusive atom fluxes among alloy constituents. Such fluxes produce topological and chemical short-range order that minimizes free-energy differences between the sub-cooled melt and the crystalline phase, and results in low levels of free volume in the sub-cooled melt at the glass-transition range. These have all proved to be important factors for glass formability. Detailed studies up to the present have demonstrated that many of these requirements are not independent but emanate from a need for efficient atomic packing in the sub-cooled melt, in which an important factor is the atomic-size mismatch among the alloy constituents.

1.3 Atomic packing in disordered metallic solids

The atomic packing in disordered solids was investigated first by Bernal (1964), who considered the problem in the context of a model of a simple liquid that consisted of randomly close-packed hard spheres of uniform size and described the structure as a distribution of five different canonical polyhedra with well-defined volume fractions.

A more realistic computer model of a disordered solid considering both attractive and repulsive atom interactions, carried out by Finney (1970), gave very similar results, establishing that the hard-sphere repulsive interactions did indeed play a dominant role in the dense random packing of atoms. While these pioneering models for liquids transforming into disordered solids gave reasonable agreement between the structure of the models and the radial distribution functions (RDFs) of atom positions of simple liquids (Bernal 1964), they severely underpredicted the densities of liquids at melting (or by extension, the densities of

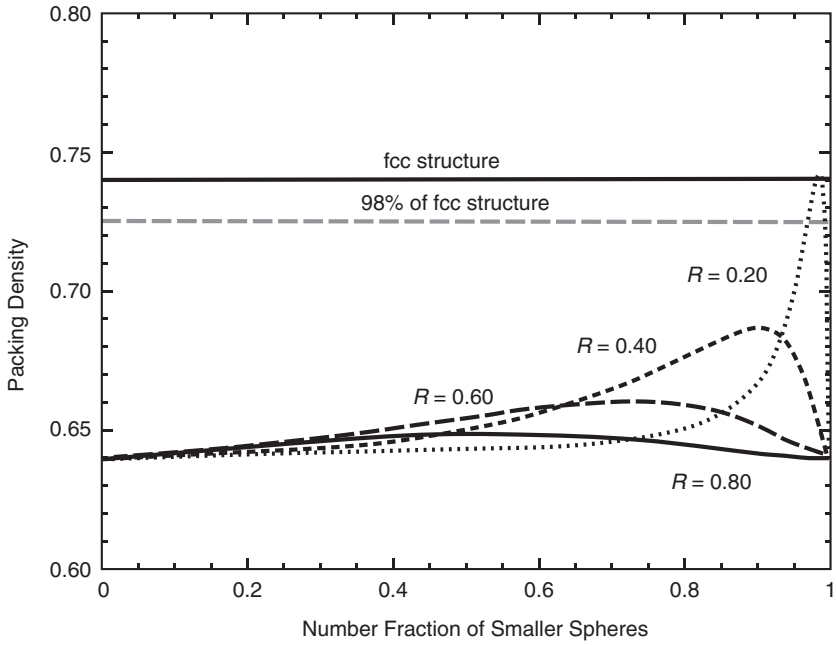

Fig. 1.1 Relative atomic packing density of a binary mixture of spheres with radius ratios R ranging from 0.2 to 0.8, based on developments of Zheng *et al*. (1995) (from Miracle *et al*. (2003): courtesy of Taylor and Francis).

glasses) in comparison with face-centered cubic (fcc) crystals, at a level of a density reduction of around 13.5% (Miracle *et al*. 2003). In comparison the density reduction of fcc crystals upon melting is only, on average, 4.5% (Brandes 1983). To explain the large density difference between the models of dense randomly packed uniform-sized spheres and the actual density of metallic glasses a number of factors for more efficient packing of spheres were considered. Since the early metallic-glass compositions were of metal–metalloid type such as Au–Si, Pd–Si, and Fe–B with number ratios of 4:1 between metal and metalloid atoms at a size ratio R of around 0.7, Polk (1972) proposed that the smaller solute metalloid atoms might more nearly fit into the interstitial spaces of the metal ions, thereby achieving a higher density. However, it was soon recognized that the interstitial volumes between metal atoms in the glass are far too small to accommodate the metalloid atoms without a large misfit strain. A number of more complete packing exercises for spheres of different size ratios R between solute (metalloid) and solvent (metal) atoms in binary systems (Visscher and Bolsterli 1972; Zheng *et al*. 1995; Lee *et al*. 2003) showed conclusively that atomic-size differences between constituents in the framework of dense random packing of hard spheres could not by themselves account for the larger density difference between actual metallic glasses and models. This is well demonstrated in Fig. 1.1, showing that the packing density of 0.64 of the models of dense randomly packed uniform-sized

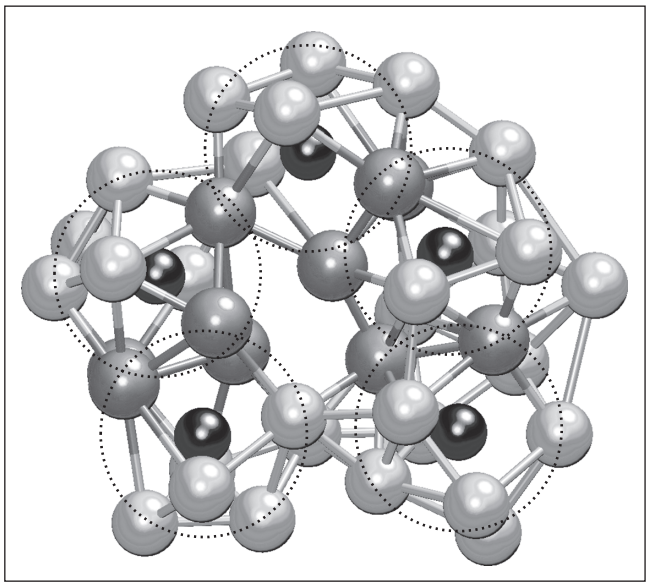

Fig. 1.2 Model of solute-centered icosahedral type atom packing in an $Ni_{80}P_{20}$ binary glass obtained through Monte Carlo modeling (from Sheng *et al*. (2006): courtesy of *Nature*).

spheres remains well below the density of 0.74 of an fcc crystal, for all reasonable number fractions of smaller solute atoms in binary alloys for all atom ratios R down to 0.4 (Miracle *et al*. 2003). In a comprehensive study Egami and Waseda (1984) calculated critical solute-concentration limits that were based on determination of excess enthalpies of binary systems through evaluation of the elastic misfit interactions between solute and solvent atoms before phase separation occurs. However, this led to no further improvement in accounting for the density disparity. The failure of these considerations resulted, in time, in a recognition that the dense random-packing models of spheres do not represent the atom packing in metallic glasses even when actual flexibility of atoms is considered and that there must be quite considerable short-to-medium-range packing order of atoms that results in the relatively high actual densities of metallic glasses. Thus, from combined modeling and experimental structural studies of Miracle *et al*. (2003), Miracle (2004a, 2004b, 2006), and Ma and co-workers (Sheng *et al*. 2006), among others, it has emerged that a high degree of short-to-medium-range atomic order exists in metallic-glass alloys. In alloys with a primary solvent component and one or more solute components the principal packing order is in the form of solute-centered polyhedra for all solute-to-solvent radius ratios R in the range 0.7–1.3. An excellent example of this is shown in Fig. 1.2, namely an $Ni_{80}P_{20}$ binary glass where the principal solute (P) appears as the small black spheres surrounded by solvent Ni atoms (dark gray) in the first icosahedral-type shells. The light-gray spheres represent, in turn, Ni atoms shared by neighboring solute atoms lying in shells outside those depicted in the figure (Sheng *et al*. 2006). In alloys with other solute components, the latter also either form additional

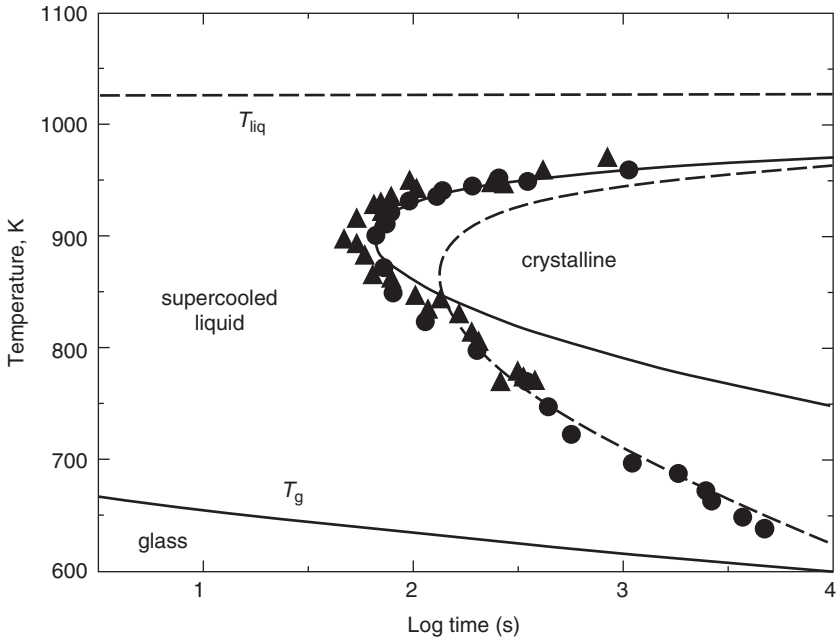

Fig. 1.3 A time–temperature–transformation diagram for the Vitreloy 1 glass-forming liquid (▲, obtained using electrostatic levitation; •, obtained using carbon crucibles) (from Busch (2000): courtesy of TMS).

polyhedral shells in which these solutes are surrounded by other solvent Ni atoms, or the additional solute atoms are preferentially accommodated in the interstitial spaces of the solute-centered polyhedral shells (Miracle 2006). While there is very good evidence for this icosahedral-type packing order (Sheng *et al*. 2006), it is not based only on purely geometrical effects of fit of atoms of different size ratios R but also arises because the free energy of the alloy is governed importantly by the concentrations of the misfit-produced elastic strain energies of atoms in the ordered polyhedral shells. The latter effects have been considered by Egami and Waseda (1984) to lead to estimates of limits to the composition of glasses provided by specific constituents. It is clear that the short-to-medium-range order that is present in the sub-cooled melt is accentuated with decreasing temperature as the elastic misfits are systematically reduced as much as possible by diffusional exchanges of atoms. The existing evidence suggests that, e.g., in the most stable Zr-based bulk metallic glass alloys the atomic ordering results in an increase in density and a decrease in free volume in the alloy to a fractional concentration of a mere 1%–2% just prior to reaching the glass transition where the kinetics of atomic ordering decreases below a critical low level (Busch 2000). It is this form of ordering that results in the very significant decrease in atomic mobility and increase in viscosity of the sub-cooled melt that suppress crystallization in these alloys. This is demonstrated well in Fig. 1.3 with the classical TTT diagram of the Zr-based alloy Vitreloy-1 ($Zr_{41.2}Ti_{13.8}Cu_{12.5}Ni_{10}Be_{22.5}$). Figure 1.3 introduces a

number of important kinetic concepts, which we develop further in more detail in subsequent sections. These include the equilibrium *liquidus temperature* T_{liq} below which, depending on time or cooling rate, a number of different scenarios can develop. For short periods of time or higher cooling rates a *supercooled liquid* is maintained in which the viscosity increases monotonically as the temperature decreases. For longer periods of time or lower cooling rates polymorphic *crystallization* sets in. The border between the supercooled liquid and initiation of crystallization is given by the characteristic "C"-shaped curve which has a *critical nose* at a location of 895 K and 60 s. Cooling rates faster than those that merely graze the nose of the curve maintain the supercooled liquid to lower temperatures, albeit with continued monotonic increase in viscosity. Finally, depending on the cooling rate, the atomic mobility in the supercooled liquid becomes too low to permit further structural relaxation and atomic compaction at the given rate of cooling. Then, the supercooled liquid undergoes a *glass transition* at T_g that is higher the higher the cooling rate, below which the excess volume per atom, the *free volume*, decreases only very sluggishly. The rather long transformation time window of 60 s at the nose permits comfortable cooling rates in the range of 1.0 K/s to avoid incipient crystallization for many processing histories for such stable glasses. The temperature dependence of the viscosity of this alloy in its supercooled liquid region is shown in Fig. 1.4 (Masuhr *et al*. 1999). The figure also shows the viscosities of many pure metals at their melting points near the bottom. These viscosities are typically three orders of magnitude lower than that of the Vitreloy 1 alloy, demonstrating why crystallization is extremely rapid in pure metals upon quenching and the extreme difficulty for them to undergo a successful glass transition. The vertical, upward-directed arrow in Fig. 1.4 shows where the glass transition occurs, at a viscosity of 10^{12} Pa s, but that some fluid-like behavior still persists at lower temperatures and higher viscosities.

1.4 Energetic characterization of the structure of metallic glasses

1.4.1 The atomic site stress tensor

A very important form of characterization of the structural state of disorder in a glass is through the atomic site stress tensor introduced by Egami and Vitek (1983). While all atoms in a crystal are in mechanical equilibrium in their orderly arrangement that results in a low internal energy, in a glass all atoms are also in mechanical equilibrium but experience very large misfit-induced forces of interaction with their neighbors. This permits one to define an atomic site stress tensor $\boldsymbol{\tau}$ resulting from the very substantial local interaction forces between atoms. Two scalar invariants of this stress tensor, defined for every atomic site, namely the atomic site pressure, p, and the atomic site deviatoric stress, $\overline{\sigma}$, are of most interest. They are defined as

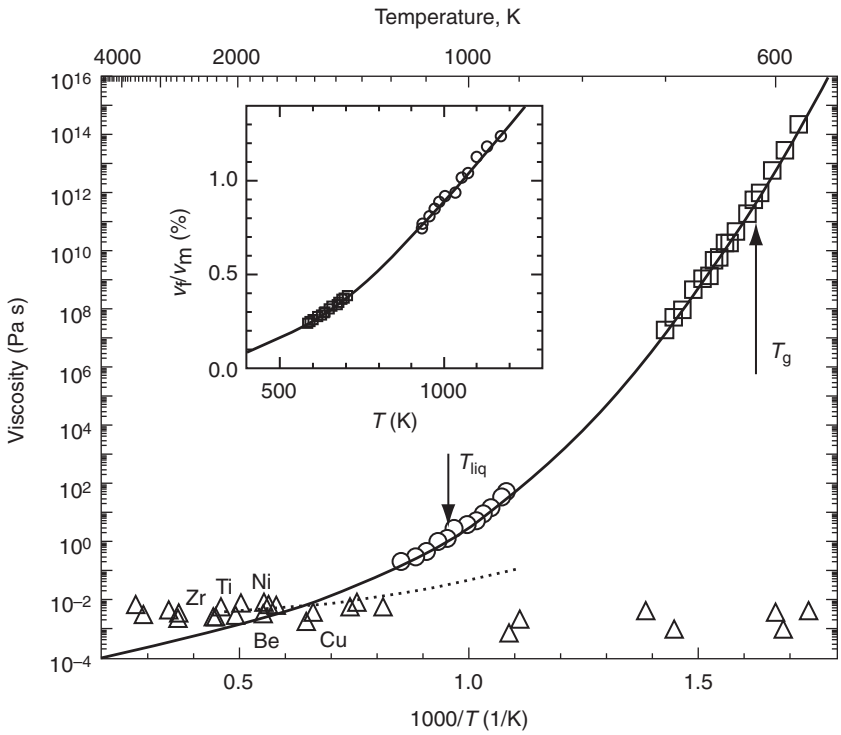

Fig. 1.4 The temperature dependence of the thermal equilibrium viscosity of liquid Vitreloy 1 compared with experimental data from viscosity experiments (○), and beam-bending experiments (□). The inset gives the temperature dependence of the free volume of this alloy. The viscosities of many pure metals (△), including Zr, Ti, Ni, Be, and Cu, are shown close to the temperature axis (from Masuhr *et al*. (1999): courtesy of the APS).

$$p(\boldsymbol{\tau}) = -(1/3)\mathrm{tr}(\boldsymbol{\tau}) \tag{1.1}$$

and

$$\overline{\boldsymbol{\sigma}}(\boldsymbol{\tau}) = -|\boldsymbol{\tau} - (1/3)\mathrm{tr}(\boldsymbol{\tau})\boldsymbol{I}| \tag{1.2}$$

where tr stands for the trace of the tensor $\boldsymbol{\tau}$ and $\boldsymbol{I}$ stands for the identity tensor (Demkowicz and Argon 2005a). These two quantities furnish directionless scalar measures of the size misfit and distortional misfit, respectively, of atomic sites. Figures 1.5(a) and (b) show the distributions of the atomic site pressure and deviatoric stress calculated by Egami and Vitek (1983) from a three-dimensional (3D) computational model of a well-relaxed glass. The pressure distribution is nearly symmetric by virtue of overall traction equilibrium since there are both dilated and compacted domains. However, the overall volume fraction of the dilatation somewhat dominates over the compaction because of the unsymmetrical character of the atomic binding potential around zero stress. The deviatoric stress distribution, however, is always positive by definition and by virtue of non-directionality. We note that the tail end of the pressure distribution on the negative side (i.e., positive mean normal stress) borders on levels of de-cohesion,

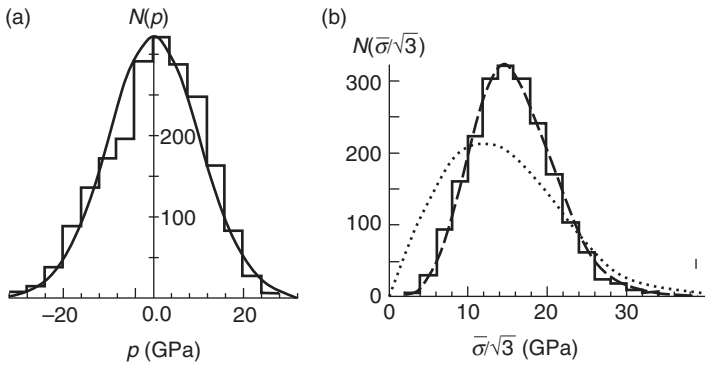

Fig. 1.5 Histogram of smoothed Gaussian distributions of (a) atomic site pressure p and (b) atomic site deviatoric stress $\bar{\sigma}$, calculated from a model of amorphous Fe (from Egami and Vitek (1983): courtesy of the Metallurgical Society of AIME).

albeit over only atomic dimensions, while the high-end tail of the deviatoric stress distribution is a large fraction of the shear modulus. These characteristics of atomic sites in glasses emphasize the very important fact that glassy solids store a very substantial excess enthalpy of disorder, which has its origin in the elastic strain energies associated with the atomic site structural misfit.

1.4.2 Calorimetry

A precise way of monitoring the thermodynamic properties of a glassy metal is accomplished through differential scanning calorimetry (DSC), in which the amount of heat required to increase the temperature of a sample is measured in comparison with that of a reference sample with well-known heat capacity. The technique supplies very useful information on the onset of property changes such as the glass transition and phase changes such as crystallization or melting as well as distinguishing thermodynamic-property differences such as levels of excess enthalpy of disorder and specific heat associated with different thermal and mechanical treatments. For example, Fig. 1.6 shows three DSC scans for a $Pd_{40}Ni_{40}P_{20}$ metallic-glass alloy heated at a rate of 20 K/min. The solid line represents the gradually increasing heat flow into an initially quenched sample as it transitions from a glassy solid into an under-cooled liquid at a glass-transition temperature of around 585 K. The dotted and dashed lines, on the other hand, show the similar endothermic transitions in samples pre-annealed at 540 K for 1.0 h and 50 h, respectively. Clearly, the much more stabilized sample with the 50 h of annealing required considerably more heat input before undergoing the transition. If crystallization had set in above the glass transition with a strong negative heat flow, as an exothermic process, a significant dip would have occurred in the scan. Alternatively, the occurrence of melting would produce a substantial upward peak (Duine *et al*. 1992).

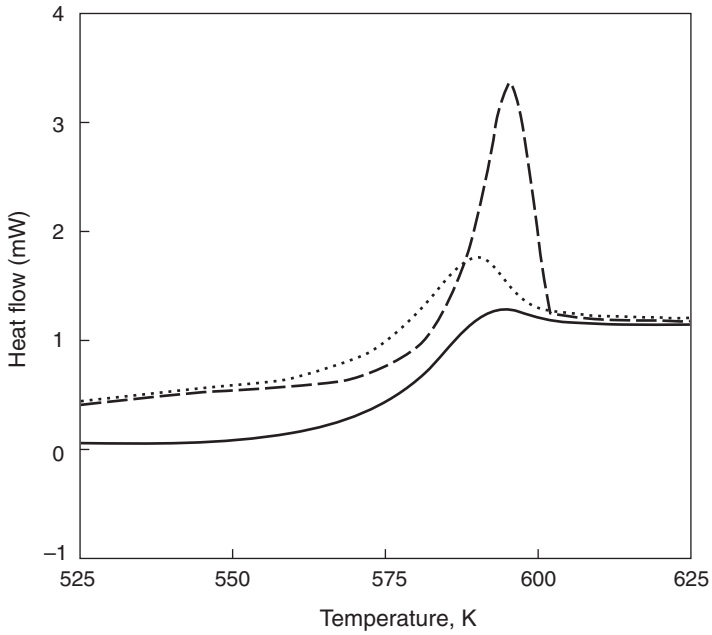

Fig. 1.6 DSC scans of thermal effects in $Pd_{40}Ni_{40}P_{20}$ with a heating rate of 20 K/min: the solid line is for a quenched sample; the dotted line and dashed lines are for samples pre-annealed at 540 K for 1.0 h and 50 h, respectively (from Duine *et al*. (1992): courtesy of Pergamon Press).

1.5 Free volume

A concept of critical importance in understanding atomic mobility in glass-forming liquids and even glasses, that is referred to as free volume, was introduced by Fox and Flory (1950), and all subsequent theoretical developments on atomic mobility in disordered structures and their structural relaxation processes have been based on this concept. In a disordered structure like a dense liquid, for an atom to migrate, room must be provided in its immediate neighborhood for it to move into. In such structures atoms occupy, on average, volumes v equal to or larger than v_0, the van der Waals volume of the atom, or its size in an ordered reference structure. When the actual size of the volume the atom occupies in the structure exceeds a critical value v_c ($v_c > v_0$), locally the excess can be considered as *free volume*. Then atomic transport occurs only when momentary voids of some critical size v^* approximately equal to the atomic volume v_0 appear by redistribution of the local free volume as a result of fluctuations. In a liquid such redistribution of free volume is considered not to require overcoming an energy barrier. Fox and Flory (1950) defined the local free volume as

$$v_f = v - v_0 \tag{1.3}$$

using v_0 rather than v_c, which needs a more precise definition that will be given below.